NACA RM L52L18

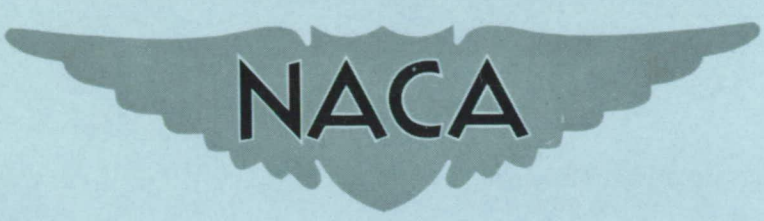


# RESEARCH MEMORANDUM

## WIND-TUNNEL INVESTIGATION OF THE STATIC LATERAL STABILITY CHARACTERISTICS OF WING-FUSELAGE COMBINATIONS AT HIGH SUBSONIC SPEEDS

ASPECT-RATIO SERIES

By Paul G. Fournier and Andrew L. Byrnes, Jr.

Langley Aeronautical Laboratory
Langley Field, Va.

Declassified December 14, 1955

NATIONAL ADVISORY COMMITTEE
FOR AERONAUTICS
WASHINGTON

February 9, 1953

NACA RM L52L18

NATIONAL ADVISORY COMMITTEE FOR AERONAUTICS

RESEARCH MEMORANDUM

# WIND-TUNNEL INVESTIGATION OF THE STATIC LATERAL STABILITY CHARACTERISTICS OF WING-FUSELAGE COMBINATIONS AT HIGH SUBSONIC SPEEDS

## ASPECT-RATIO SERIES

By Paul G. Fournier and Andrew L. Byrnes, Jr.

## SUMMARY

An investigation was conducted in the Langley high-speed 7- by 10-foot tunnel to determine the effect of aspect ratio on the static lateral stability characteristics, at high subsonic speeds, of wing-fuselage combinations having wings of 45° sweepback at the quarter-chord line and taper ratio of 0.6. The rate of change of effective dihedral with lift coefficient $C_{l_{\beta_{C_L}}}$ increased in magnitude with increasing Mach number. This result is in contrast to the slight reduction predicted by available theory. Above the force-break Mach number, $C_{l_{\beta_{C_L}}}$ exhibited a rapid decrease with increasing Mach number. The experimental variation of $C_{l_{\beta_{C_L}}}$ with aspect ratio was found to have the same trend as that indicated by theory but the values are more negative than those predicted. The rate of reduction of $C_{l_{\beta_{C_L}}}$ with increasing aspect ratio is also somewhat greater than that indicated by the calculations. The fuselage accounted almost entirely for the measured values of the derivatives of yawing moment due to sideslip $C_{n_\beta}$ and lateral force due to sideslip $C_{Y_\beta}$ at the lower lift coefficients.

## INTRODUCTION

A systematic research program is being carried out in the Langley high-speed 7- by 10-foot wind tunnel to determine the aerodynamic characteristics of various arrangements of the component parts of research

models, including some complete model configurations. Data are being obtained on characteristics in pitch and sideslip and during steady roll at Mach numbers from 0.40 to about 0.95. The Reynolds number range for the sting-supported models varies from $1.5 \times 10^6$ to $5.0 \times 10^6$, depending on the wing plan form and the test Mach number.

This paper presents results which show the effect of aspect ratio on the aerodynamic characteristics in sideslip of wings having a sweep angle of $45^\circ$, a taper ratio of 0.6, and an NACA 65A006 airfoil section in combination with a fuselage that was common to all configurations. The pitch characteristics of these wing-fuselage combinations along with the fuselage-alone data are presented in reference 1. The effect of sweep on the aerodynamic characteristics in sideslip is presented in reference 2. In order to expedite the issuance of the results, only a limited comparison of some of the more significant characteristics with available theory is presented in this paper.

## COEFFICIENTS AND SYMBOLS

The stability system of axes used for the presentation of the data, together with an indication of the positive forces, moments, and angles, are presented in figure 1. All moments are referred to the quarter-chord point of the wing mean aerodynamic chord (fig. 2).

$C_L$ lift coefficient, Lift/qS

$C_l$ rolling-moment coefficient, Rolling moment/qSb

$C_n$ yawing-moment coefficient, Yawing moment/qSb

$C_Y$ lateral-force coefficient, Lateral force/qS

$q$ dynamic pressure, $\rho V^2/2$, lb/sq ft

$\rho$ mass density of air, slugs/cu ft

$V$ free-stream velocity, fps

$M$ Mach number

$R$ Reynolds number, $\frac{\rho V \bar{c}}{\mu}$

$\mu$ absolute viscosity of air, slugs/ft-sec

$S$ wing area, sq ft

$b$ wing span, ft

$c$ wing chord, ft

$\bar{c}$ mean aerodynamic chord, $\frac{2}{S}\int_0^{b/2} c^2 dy$, ft

$y$ spanwise station, ft

$\alpha$ angle of attack, deg

$\beta$ angle of sideslip, deg

$\delta$ deflection, ft

$C_{l_\beta} = \frac{\partial C_l}{\partial \beta}$ per deg

$C_{n_\beta} = \frac{\partial C_n}{\partial \beta}$ per deg

$C_{Y_\beta} = \frac{\partial C_Y}{\partial \beta}$ per deg

$C_{l_{\beta_{C_L}}} = \frac{\partial C_{l_\beta}}{\partial C_L}$

Subscript:

WF-F wing-fuselage values minus fuselage values

## MODEL AND APPARATUS

The wing-fuselage combinations tested are shown in figure 2 and are the same wing-fuselage combinations used in reference 1. All wings had an NACA 65A006 airfoil section parallel to the fuselage center line and were attached to the fuselage in a midwing position. All wings were constructed of solid aluminum alloy except the aspect-ratio-4 wing which was of composite construction, consisting of a steel core and a bismuth-tin covering. The aluminum fuselage was common to all configurations; the ordinates are presented in reference 1.

The three wings used in this investigation represent a part of a family of wings being studied in a more extensive program; therefore, the wing designation system described in reference 1 is being utilized. For example, the wing designated by 45-4-0.6-006 has the quarter-chord line swept back 45°, an aspect ratio of 4, and a taper ratio of 0.6. The number 006 refers to the section designation; in this case the design lift coefficient is zero and the thickness is 6 percent of the chord.

The models were tested on the sting-support system shown in figures 3 and 4. With this support system, the model can be remotely operated through an angle range of 28° in the plane of the vertical strut. By utilization of couplings in the sting behind the model, the model can be rolled through 90° so that either angle of attack (fig. 3) or angle of sideslip (fig. 4) can be the remotely controlled variable. With the model horizontal (fig. 3), couplings can be used to support the model at angles of sideslip of approximately -4° and 4° while the model is tested through the angle-of-attack range. The forces and moments were measured about the aerodynamic centers of the respective wings by an electrical strain-gage balance housed in the fuselage of the model.

## TEST AND CORRECTIONS

The tests were conducted in the Langley high-speed 7- by 10-foot tunnel through a Mach number range from approximately 0.40 to 0.95. The size of the models used caused the tunnel to choke at corrected Mach numbers of from 0.95 to 0.96, depending on the wing being tested. The blocking corrections which were applied were determined by the velocity-ratio method of reference 3.

Two groups of tests were made. The first group, from which the bulk of the data was obtained, was run at angles of sideslip of -4° and 4° through an angle-of-attack range of -3° to 24° (fig. 3). In addition, tests were made at several selected angles of attack through a sideslip angle range of 4° to -10°.

The jet-boundary corrections which were applied to angle of attack were determined from reference 4. The corrections to lateral force, yawing moment, and rolling moment were considered negligible. Tare values were determined but were found to be negligible and therefore were not applied. The angles of attack and angles of sideslip have been corrected for the deflection of the sting-support system and balance under load.

Under the action of an aerodynamic lift load, the wings assumed a curved dihedral distribution. With the model at a sideslip angle, this dihedral produced a rolling moment which added to the rolling moment of

the rigid wing and increased with lift; accordingly, the method of reference 2 was used to correct the data to the rigid-wing case.

In order to approximate the dihedral distribution that existed during the tests, an elliptical load distribution was simulated by applying static loads at four spanwise points along the quarter-chord line of each wing. The deflection of the wing at several spanwise points was measured by dial gages and the resulting aeroelastic dihedral curves are presented in figure 5. The distributions of the local dihedral angle $\Gamma'$ were determined by measuring the slope of these curves at several spanwise stations. An equivalent dihedral angle was evaluated and was used to calculate the correction increment $\Delta C_{l_{\beta C_L}}$ for the wings with aspect ratios of 4 and 6. These corrections are presented in figure 6. The correction for the aspect-ratio-2 wing was found to be negligible. A more complete discussion of these corrections, including the formulas, is presented in reference 2.

The variation of Reynolds number (based on the mean aerodynamic chord of the respective wings) with test Mach number is presented in figure 7.

## RESULTS AND DISCUSSION

The basic data for the wing-fuselage configurations having wings of aspect ratio 2 and 6 are presented in figures 8 and 9, respectively. The basic data for the configuration with an aspect-ratio-4 wing are presented in reference 2. These data have not been corrected for aeroelastic distortion. The bulk of the data was obtained from tests at angles of sideslip of $-4^\circ$ and $4^\circ$. The flagged symbols (figs. 8 and 9) represent results from the small number of tests in which the angle of sideslip was the variable.

The basic data for the fuselage alone were presented in reference 2, where it was shown that Mach number variations within the test range have little effect on the fuselage-alone parameters.

A sample of the data obtained through the sideslip-angle range was presented in reference 2. The slight nonlinearity indicated over the sideslip-angle range could be attributed almost entirely to the fuselage in that both the fuselage-alone and the wing-fuselage combinations showed about the same degree of nonlinearity.

Rolling moment due to sideslip.- The effect of aspect ratio on the variation of the effective dihedral parameter $C_{l_\beta}$ with lift coefficient

for the wing-fuselage configurations is presented in figure 10. The wing plus wing-fuselage interference data (fig. 11) for the same conditions (obtained by subtracting the fuselage-alone data of ref. 2 from the data of fig. 10) show the same trends as the wing-fuselage data. The fuselage-alone data of reference 2 were corrected to the proper wing geometry and the subtractions were made at corresponding angles of attack.

At low lift coefficients, the rate of change of $C_{l_\beta}$ with lift coefficient decreases with increasing aspect ratio up to the force-break Mach number. In general, the maximum negative value of $C_{l_\beta}$ reached for each wing increased with increasing Mach number. The range of lift coefficients over which the variation is linear changes very little over the aspect-ratio range investigated. For all wings, however, the linear range increases with increasing Mach number. It should be noted that in these tests the Reynolds number necessarily increased with increasing Mach number, the greater change being at Mach numbers below 0.80 (fig. 7). Therefore, some of the variation of $C_{l_\beta}$ might be attributable to Reynolds number effects. It is believed, however, that the Reynolds number variations that existed in the higher range of Mach number were of little significance in comparison with the effects of Mach number.

The variation of the slope $C_{l_{\beta_{C_L}}}$ at zero lift (with and without aeroelastic correction applied) with Mach number is presented in figure 12 and the variation with aspect ratio is presented in figure 13. The theoretical values were computed by the method of reference 5 and corrected for the effects of Mach number by the method of reference 6. The experimental data corrected for aeroelastic distortion indicate an increase in the absolute value of $C_{l_{\beta_{C_L}}}$ with increasing Mach number up to the force break, as had been found for two of the three wings presented in reference 2. The available theory invariably indicates a slight decrease in $C_{l_{\beta_{C_L}}}$ with increasing Mach number.

The wings with aspect ratios of 2 and 4 exhibit a rapid reduction of the absolute value of $C_{l_{\beta_{C_L}}}$ with Mach number above the force-break Mach number; whereas, there was only a slight reduction in the case of the wing with an aspect ratio of 6 as the maximum test Mach number was approached. A slight increase in the Mach number at which $C_{l_{\beta_{C_L}}}$ began to decrease resulted from increasing the wing aspect ratio. It may be

noted in reference 1 that the drag-rise Mach number also tended to increase slightly with increasing aspect ratio.

The agreement between experiment and theory, in regard to the variation of $C_{l_{\beta_{C_L}}}$ with aspect ratio (fig. 13), is only fair in that the experimental absolute values of $C_{l_{\beta_{C_L}}}$ generally are considerably larger than predicted values, particularly at the high Mach numbers. The trend with increasing aspect ratio is in general agreement with theory, although the theoretical variation is somewhat smaller than that obtained by experiment.

Yawing moment and lateral force due to sideslip.- The effect of aspect ratio on the variation of the lateral-stability parameters $C_{n_\beta}$ and $C_{Y_\beta}$ with lift coefficient is presented in figures 14 and 15 for the wing-fuselage configurations. The wing plus wing-fuselage interference data, which were obtained by subtracting the fuselage-alone data (modified for the proper wing geometry) of reference 2 from the data of figures 14 and 15, are presented in figures 16 and 17. At the lower lift coefficients, the fuselage contribution to $C_{n_\beta}$ and $C_{Y_\beta}$ accounts for about the entire measured values. (Compare figs. 14 and 15 with figs. 16 and 17.)

The breaks in the curves at the higher lift coefficients occur at approximately the same lift coefficient as the breaks in the $C_{l_\beta}$ curves and are probably due to partial stalling which changes the magnitude and orientation of the resultant force on the two wing panels.

## CONCLUSIONS

The results of the present investigation of the aerodynamic characteristics in sideslip, at high subsonic speeds, of wings having various aspect ratios, sweep angle of 45°, taper ratio 0.6, and having an NACA 65A006 airfoil section indicate the following conclusions:

1. For all wings tested, the absolute value of $C_{l_{\beta_{C_L}}}$ (rate of change of the effective dihedral with lift coefficient) generally increased as the Mach number increased to the force-break value, although available theory indicates that a slight decrease in this parameter with increasing Mach number should be expected.

2. The experimental variation of $C_{l_{\beta_{C_L}}}$ with aspect ratio has the same trend as that indicated by the theory but the values are more negative than those predicted. The rate of reduction of $C_{l_{\beta_{C_L}}}$ with increasing aspect ratio is also somewhat higher than the calculated results.

3. At the lower lift coefficients, the experimentally determined values of $C_{n_\beta}$ (yawing moment due to sideslip) and $C_{Y_\beta}$ (lateral force due to sideslip) are due almost entirely to the fuselage for the models tested.

Langley Aeronautical Laboratory,
National Advisory Committee for Aeronautics,
Langley Field, Va.

## REFERENCES

1. Kuhn, Richard E., and Wiggins, James W.: Wind-Tunnel Investigation of the Aerodynamic Characteristics in Pitch of Wing-Fuselage Combinations at High Subsonic Speeds. Aspect-Ratio Series. NACA RM L52A29, 1952.

2. Kuhn, Richard E., and Fournier, Paul G.: Wind-Tunnel Investigation of the Static Lateral Stability Characteristics of Wing-Fuselage Combinations at High Subsonic Speeds - Sweep Series. NACA RM L52G11A, 1952.

3. Hensel, Rudolph W.: Rectangular-Wind-Tunnel Blocking Corrections Using the Velocity-Ratio Method. NACA TN 2372, 1951.

4. Gillis, Clarence L., Polhamus, Edward C., and Gray, Joseph L., Jr.: Charts for Determining Jet-Boundary Corrections for Complete Models in 7- by 10-Foot Closed Rectangular Wind Tunnels. NACA ARR L5G31, 1945.

5. Toll, Thomas A., and Queijo, M. J.: Approximate Relations and Charts for Low-Speed Stability Derivatives of Swept Wings. NACA TN 1581, 1948.

6. Fisher, Lewis R.: Approximate Corrections for the Effects of Compressibility on the Subsonic Stability Derivatives of Swept Wings. NACA TN 1854, 1949.

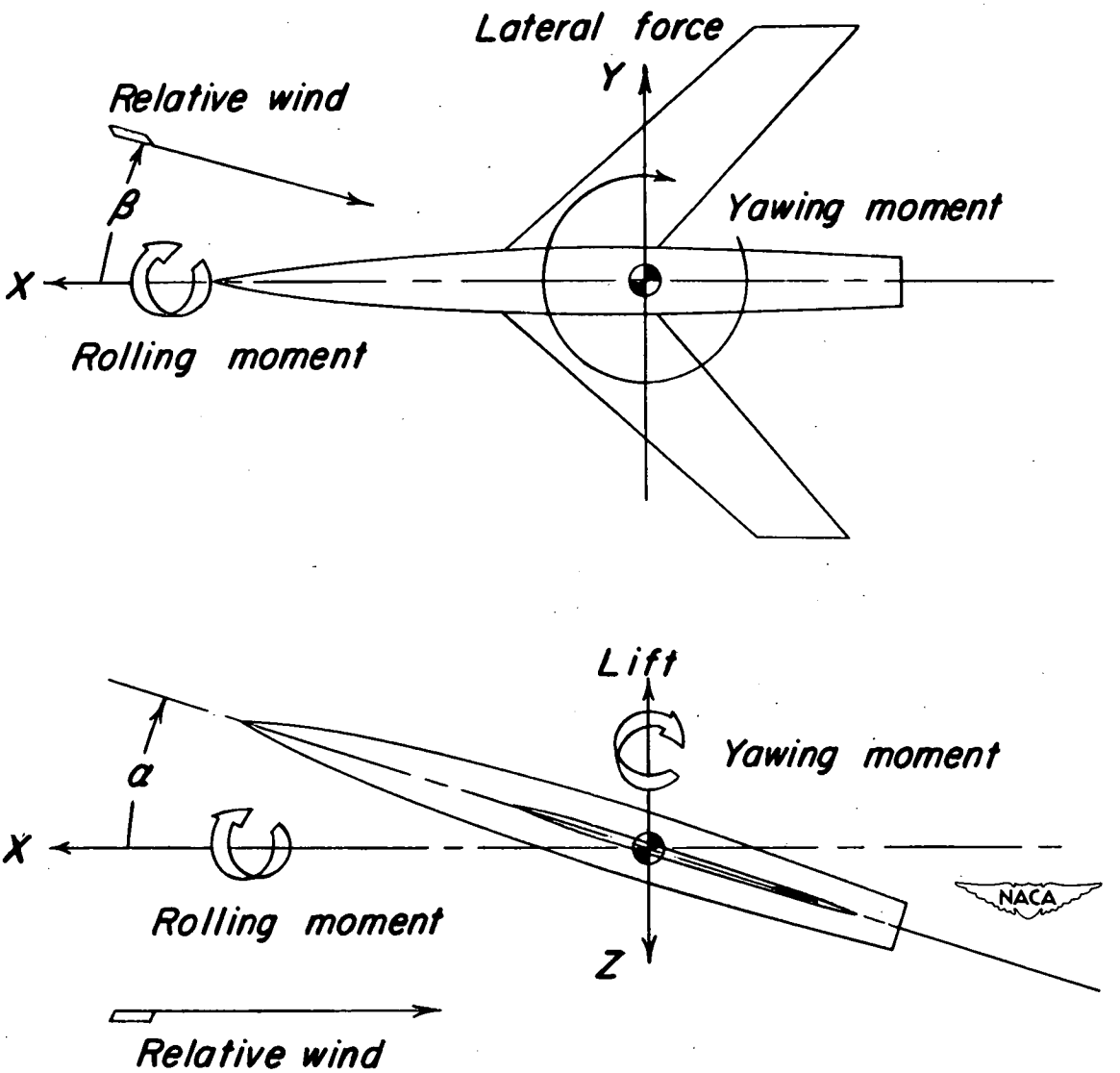


Figure 1.- System of axes used showing the positive direction of forces, moments, and angles.

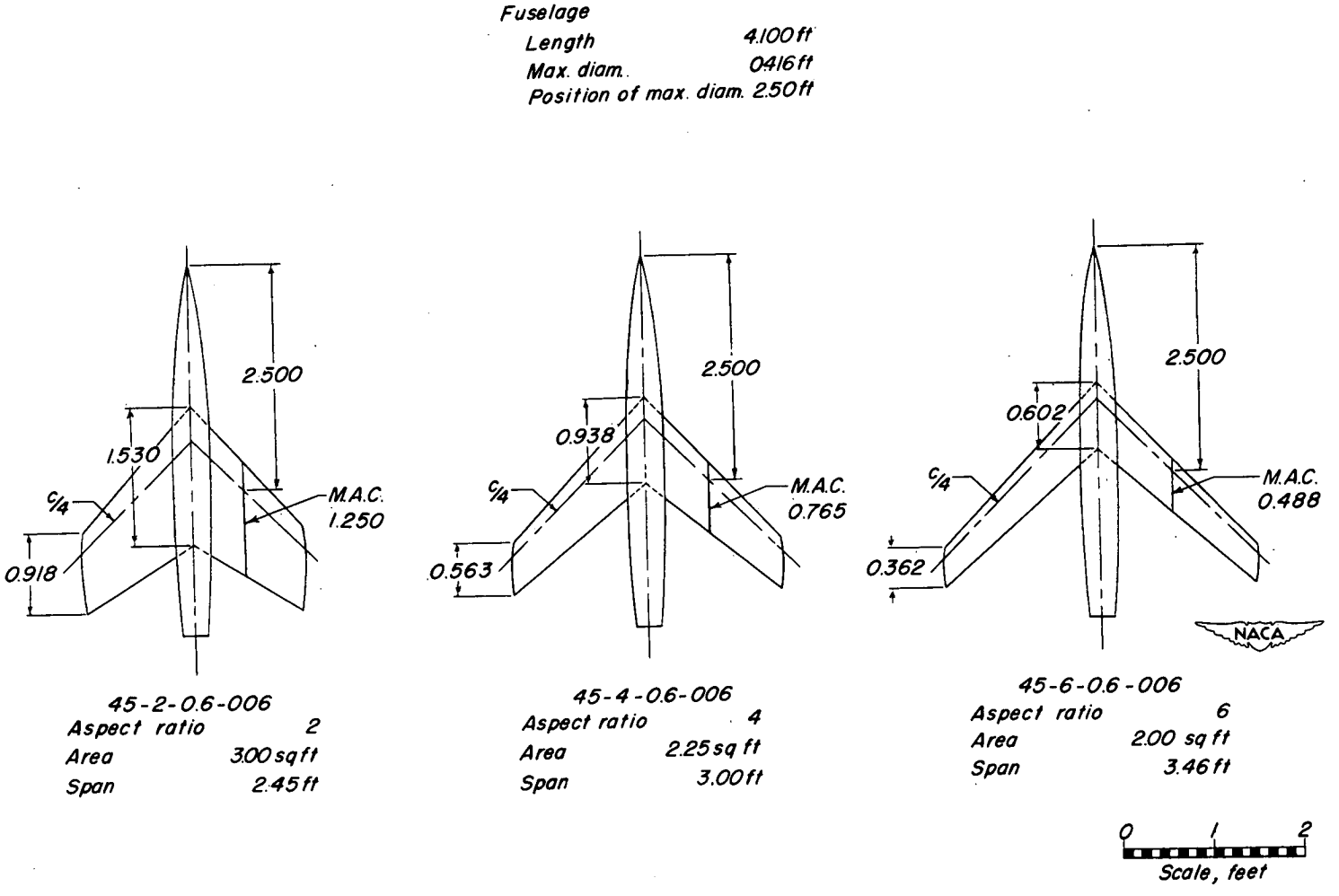


Figure 2.- Drawing of the three wing-fuselage configurations having wings of 45° sweep, 0.6 taper ratio, 0 incidence, 0 dihedral, and NACA 65A006 airfoil section parallel to the fuselage center line.

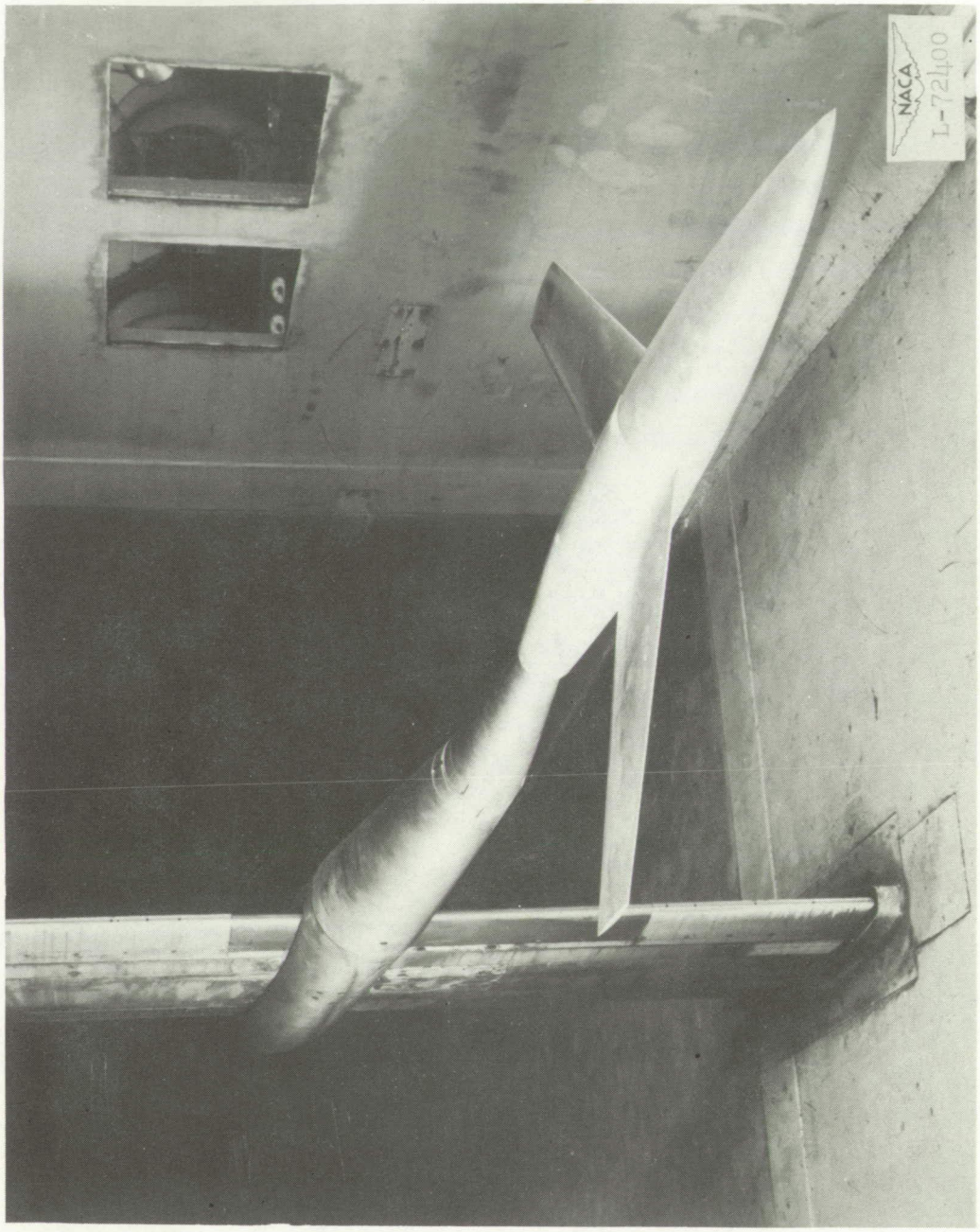


Figure 3.- A typical model installed on the sting-support system for variable angle-of-attack tests, shown at an angle of sideslip of 4°.

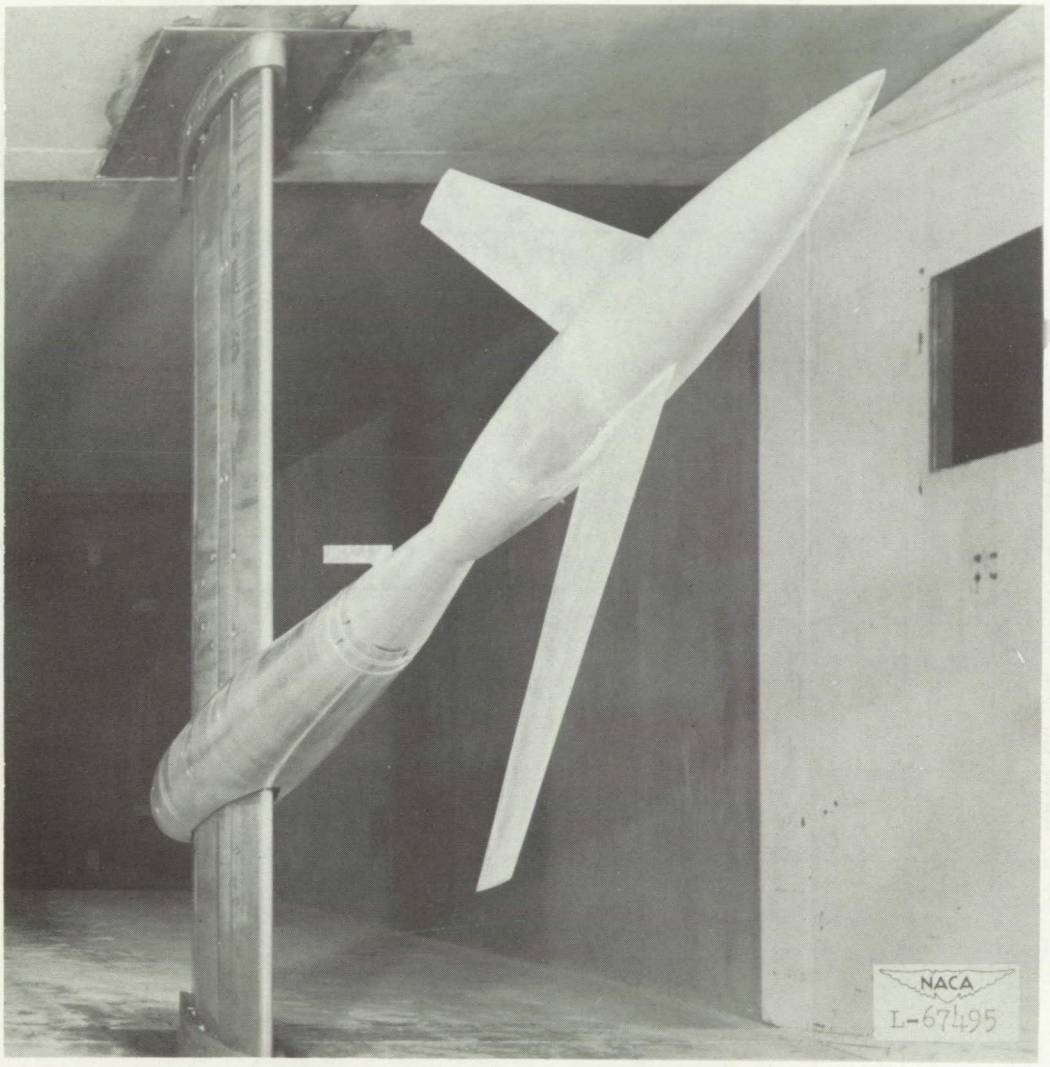


Figure 4.- A typical model installed for tests with variable angles of sideslip. Angle of attack, 0°.

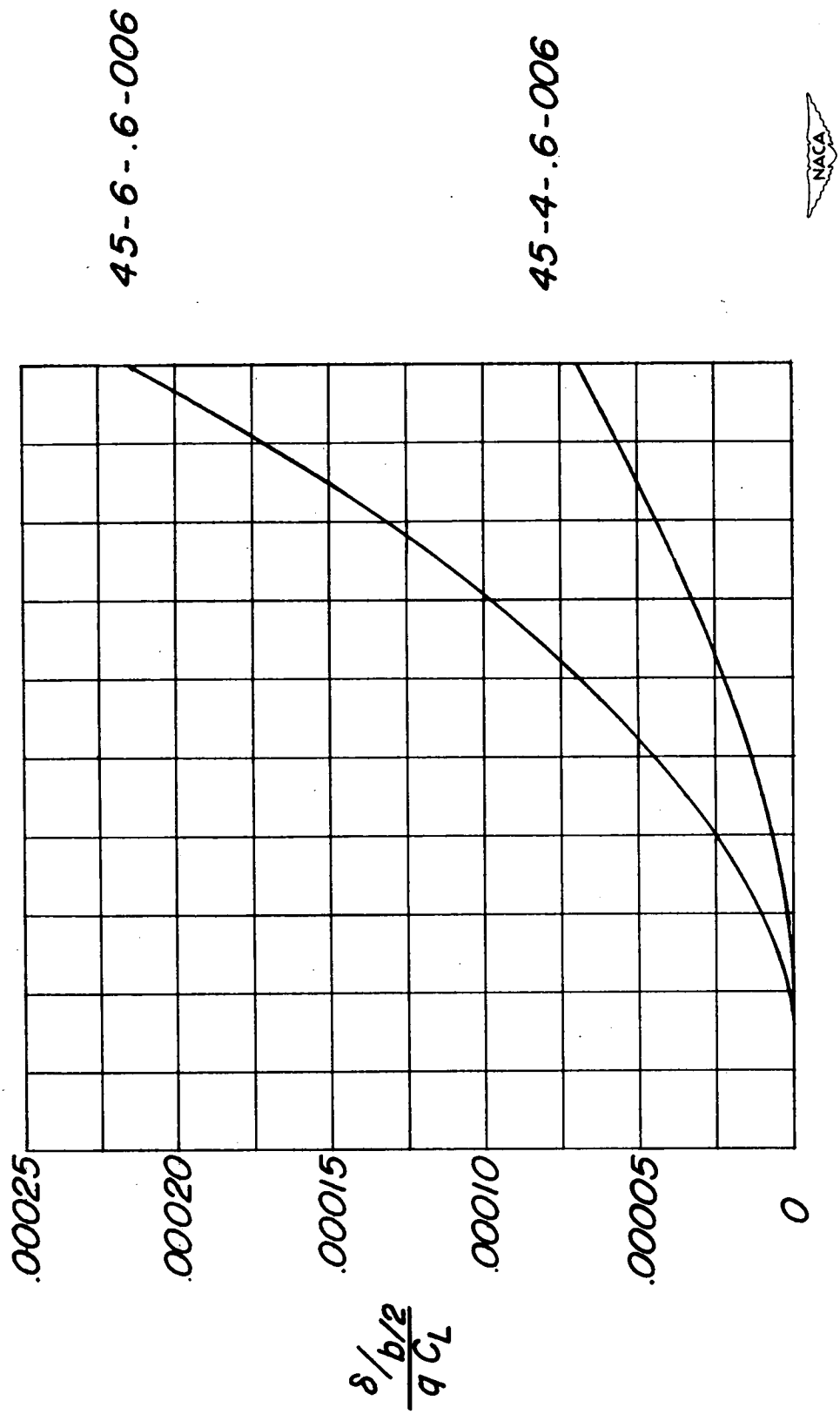


Figure 5.- Deflection curves for test wings.

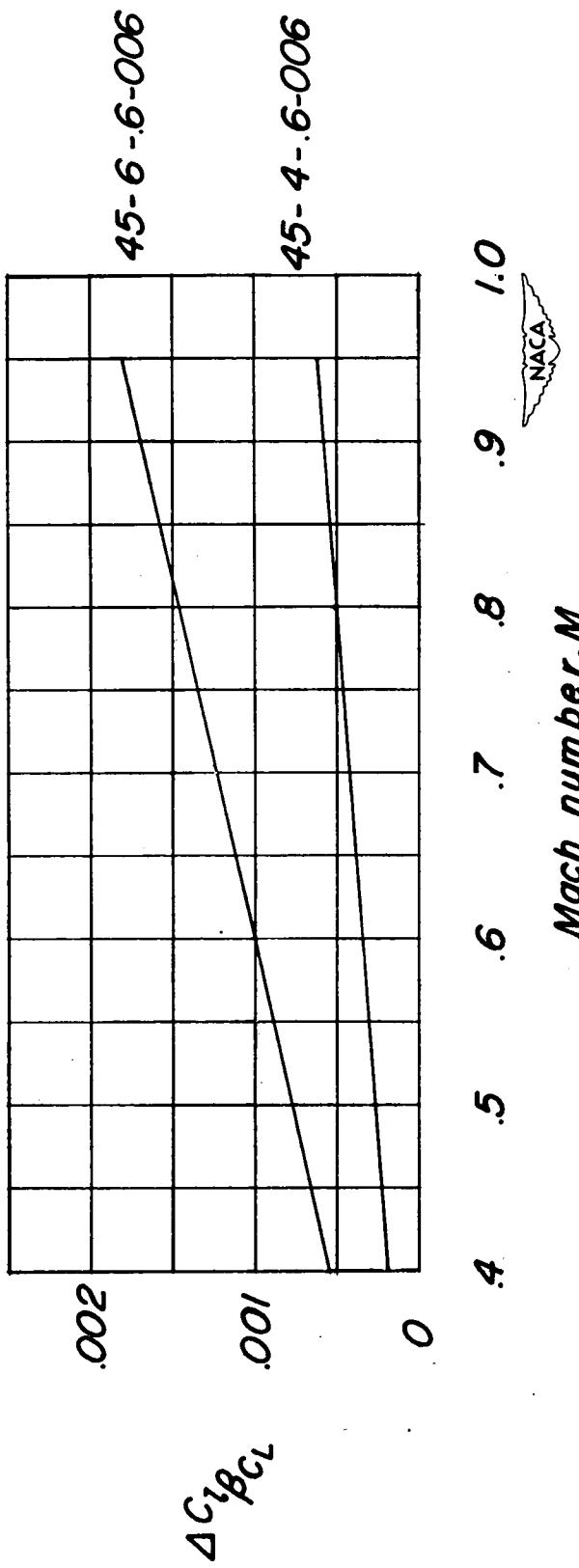


Figure 6.- Corrections for the effects of aeroelastic distortion.

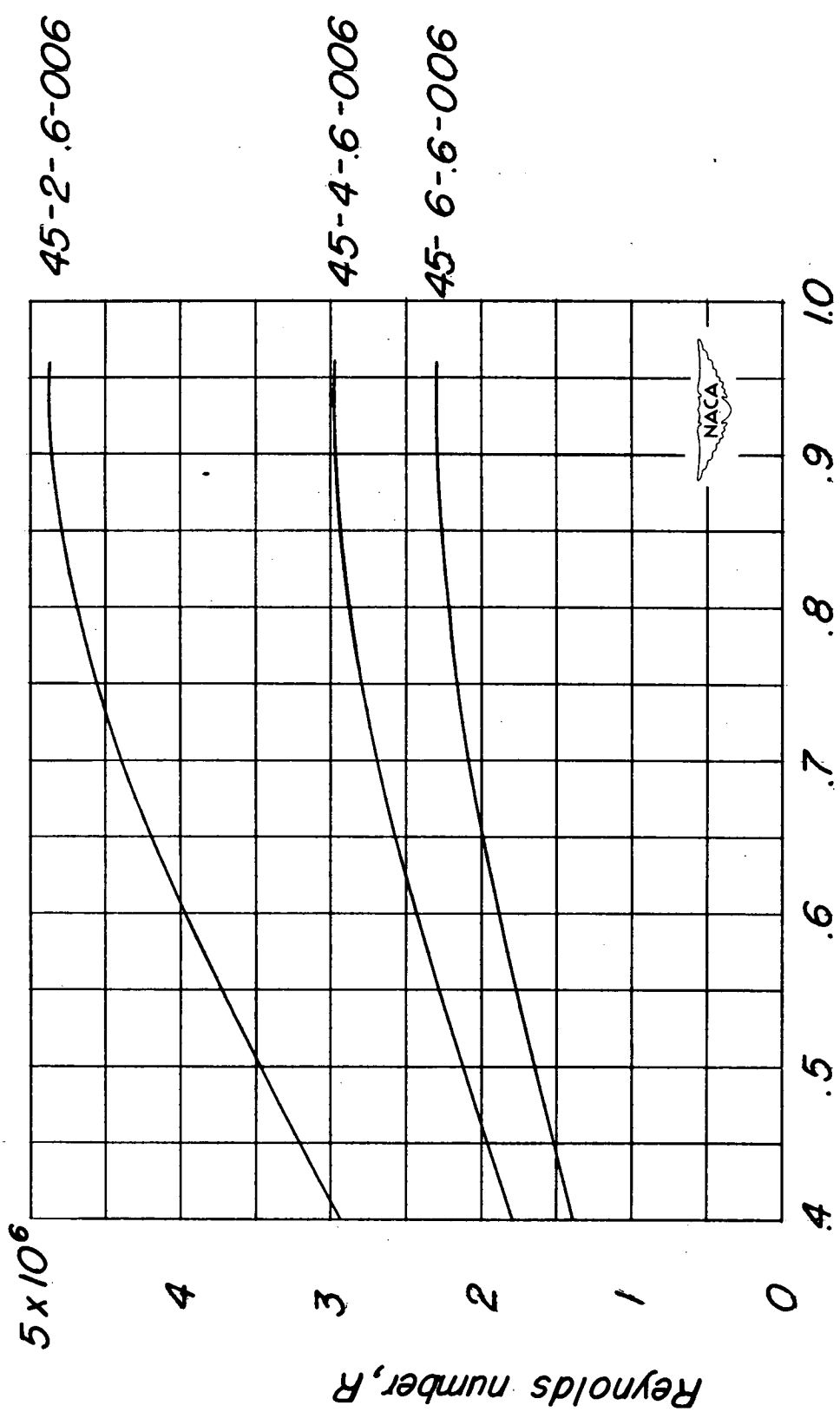


Figure 7.- Variation of mean Reynolds number with test Mach number based on the wing mean aerodynamic chord.

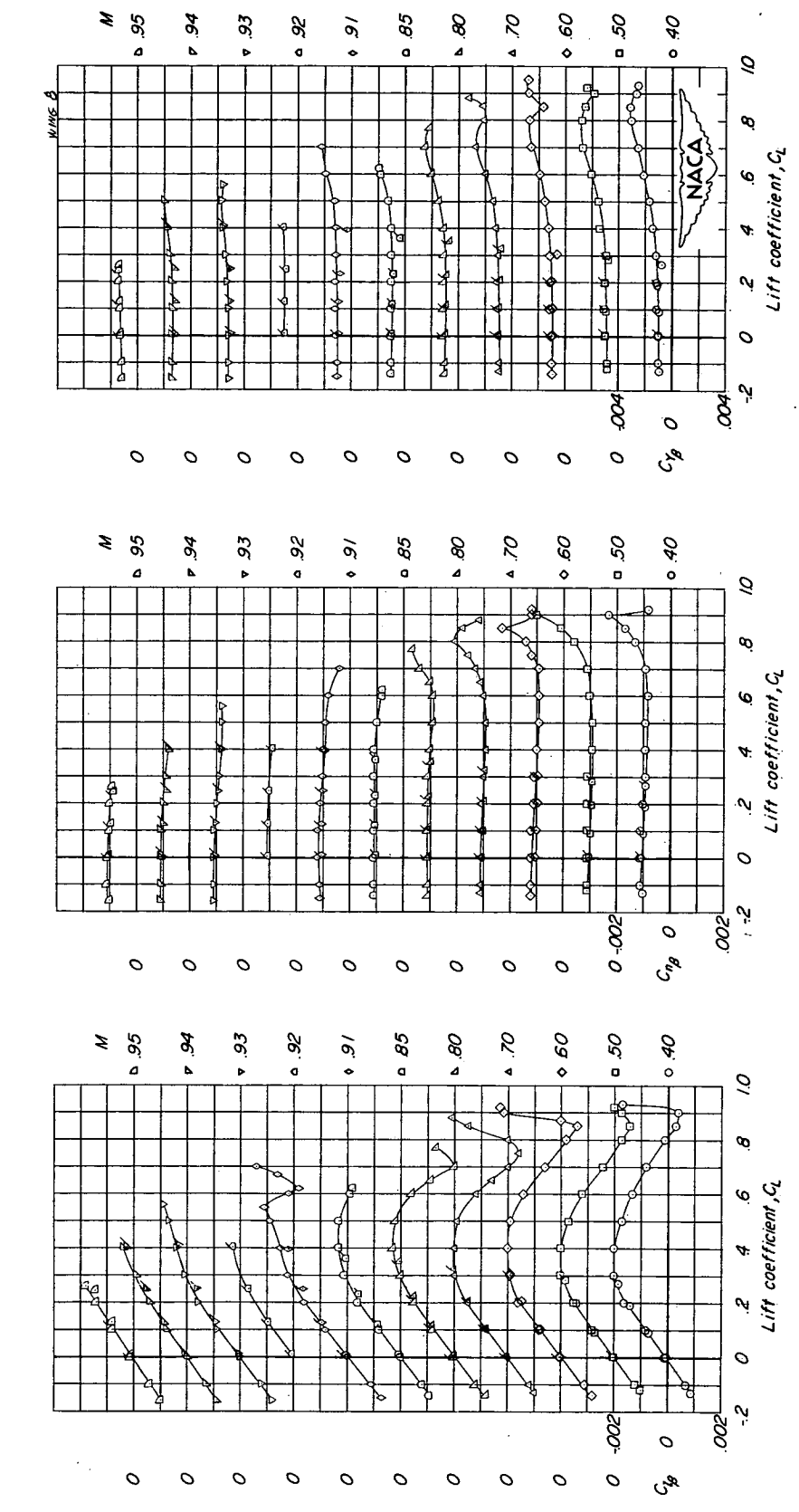


Figure 8.- Lateral stability characteristics of the 45-2-.6-006 wing-fuselage combination. Not corrected for aeroelastic distortion. Flagged symbols represent tests through the range of sideslip angles.

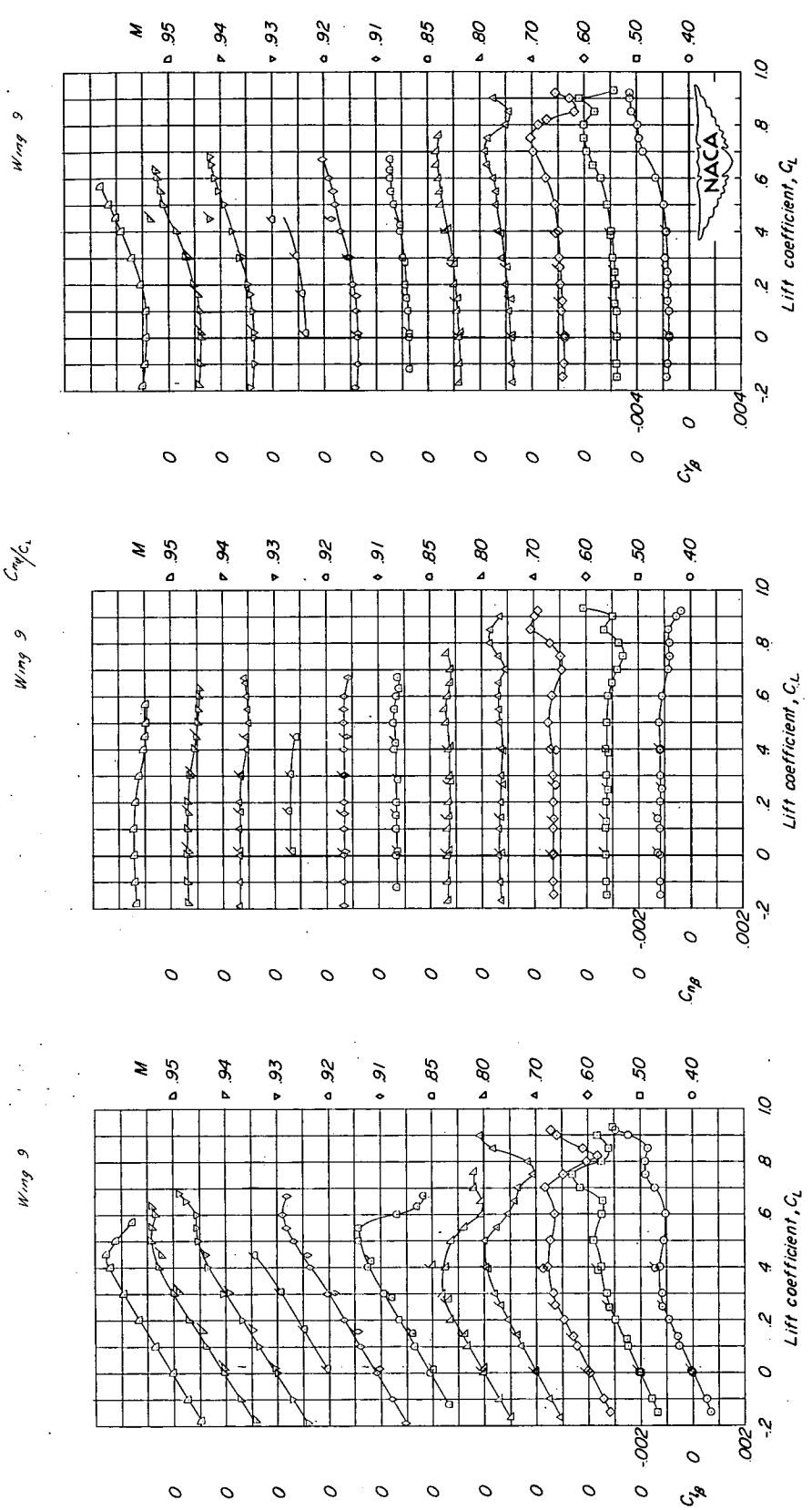


Figure 9.- Lateral stability characteristics of the 45-6-.6-006 wing-fuselage combination. Not corrected for aeroelastic distortion. Flagged symbols represent tests through the range of sideslip angles.

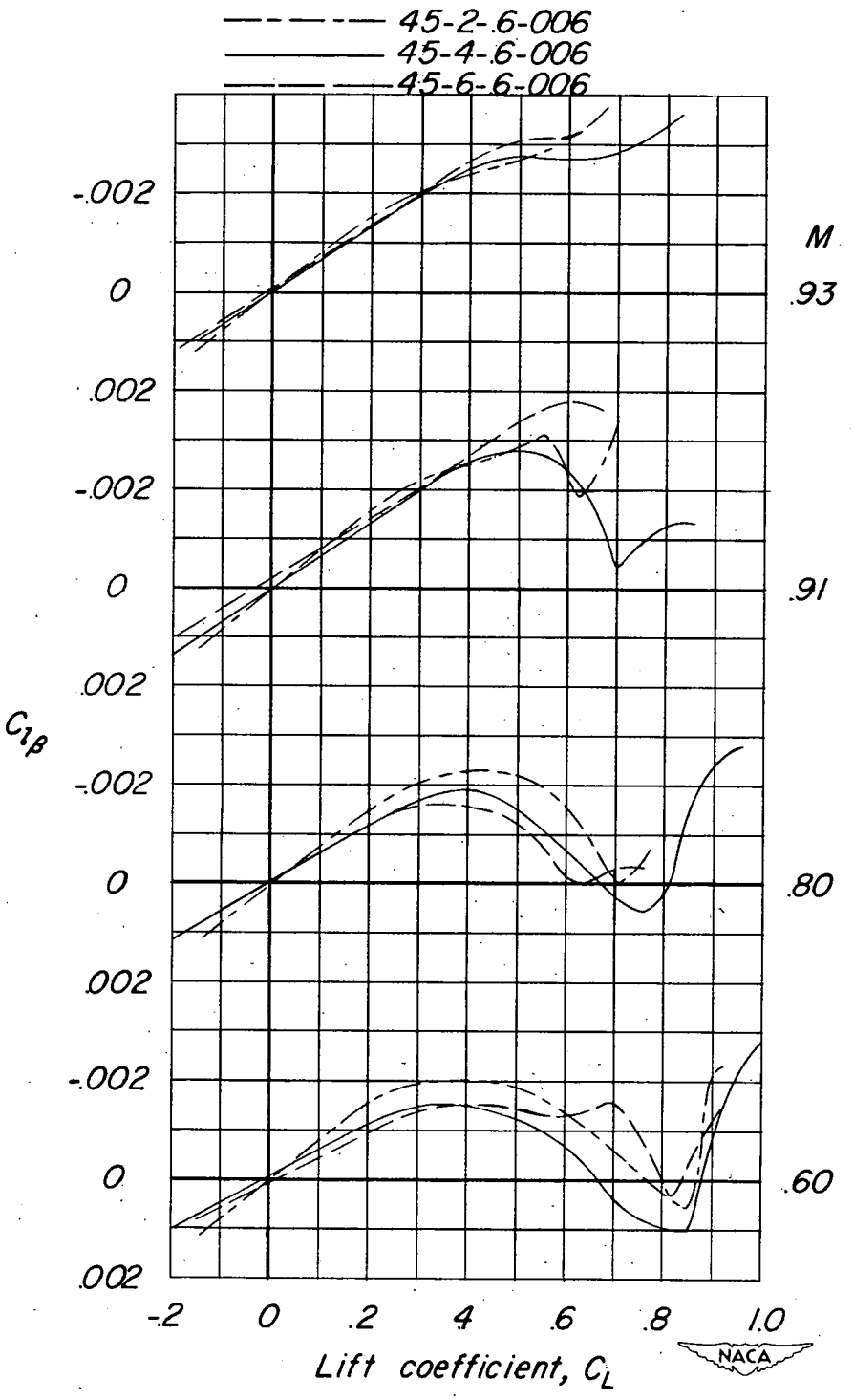


Figure 10.- Effect of aspect ratio on the variation of $C_{l_\beta}$ with lift coefficient for the wing-fuselage configurations at several Mach numbers. Not corrected for aeroelastic distortion.

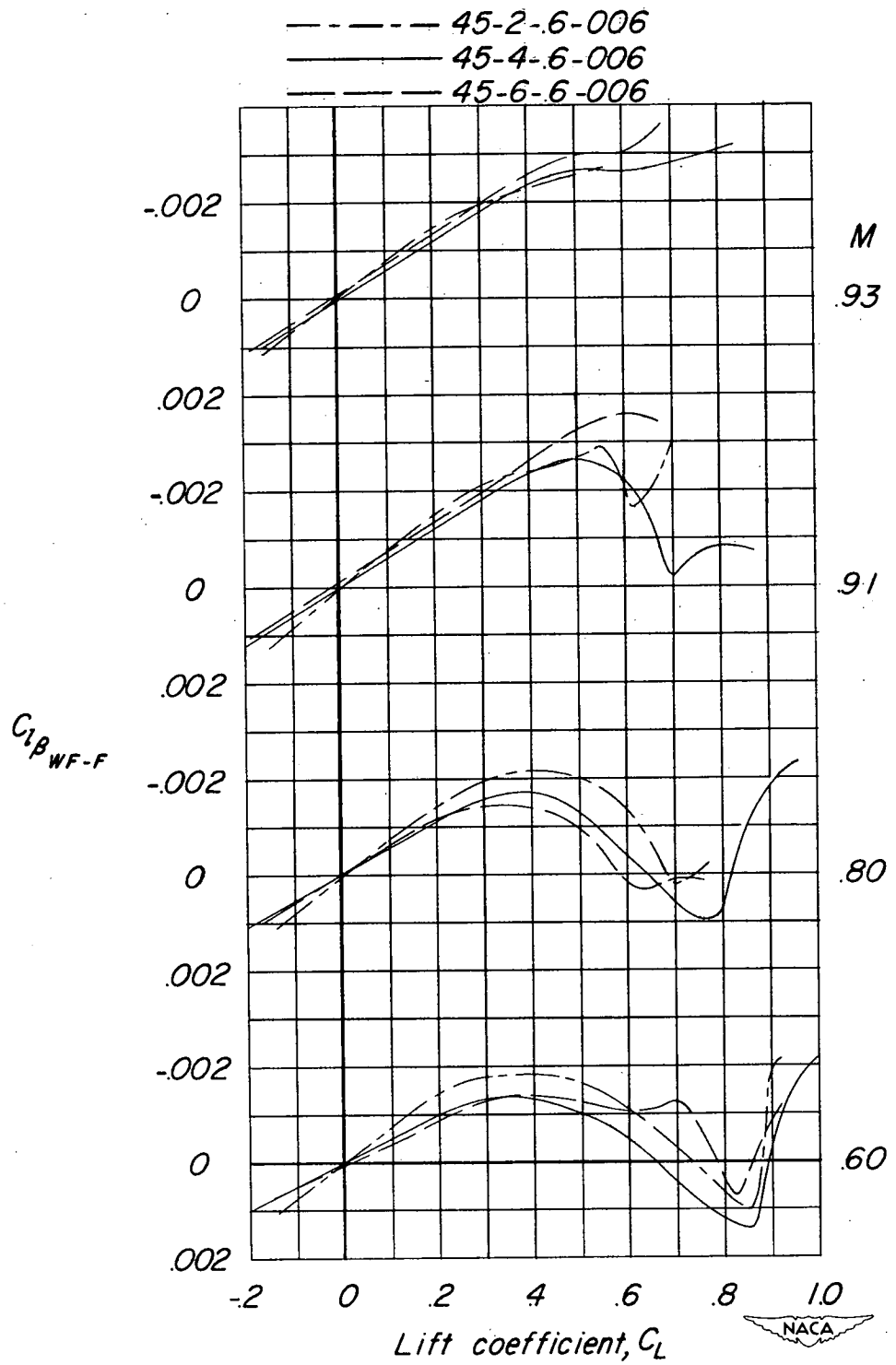


Figure 11.- Wing-plus-wing-fuselage-interference values of $C_{l_\beta}$ for the test wings compared at several Mach numbers. Not corrected for aeroelastic distortion.

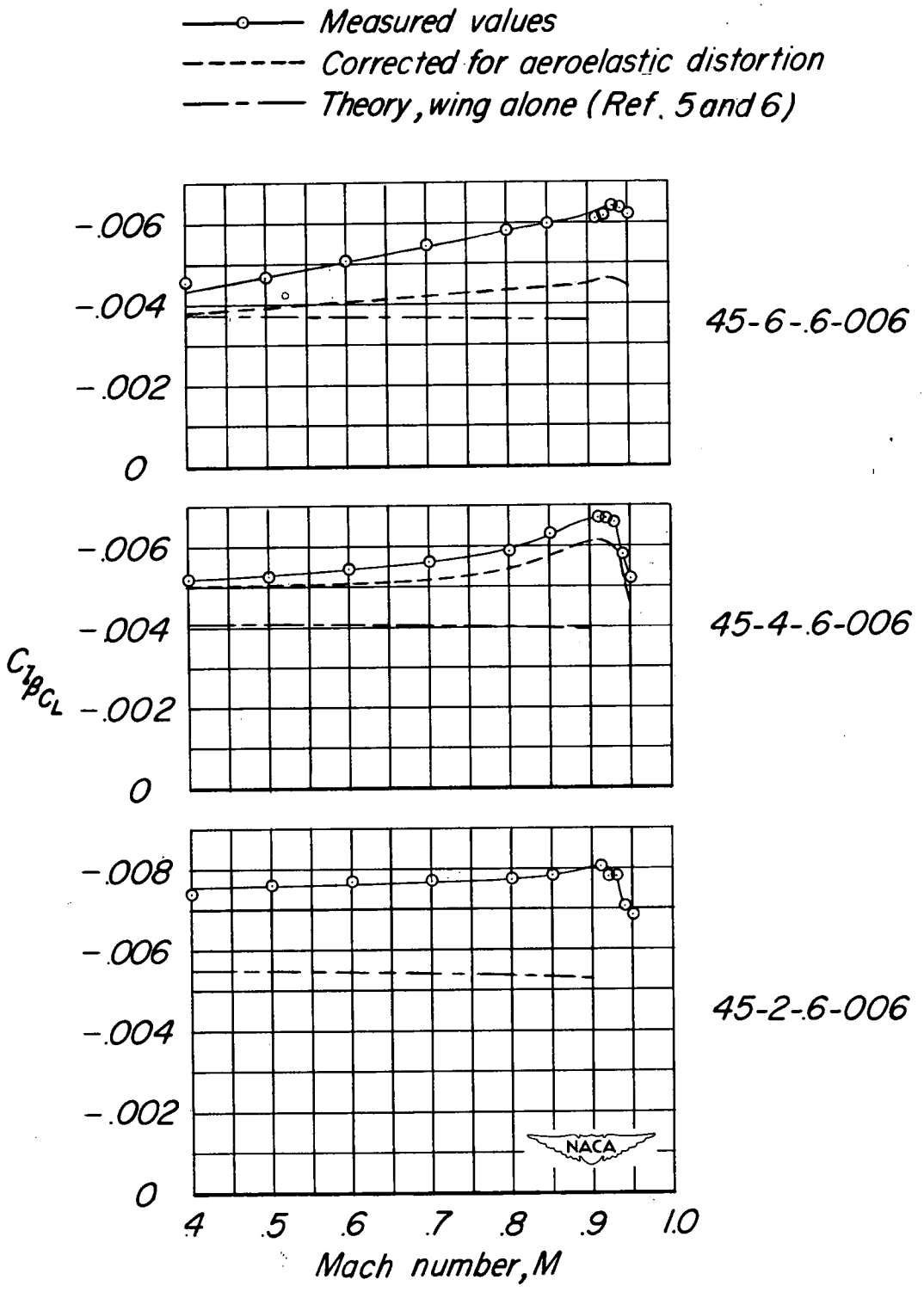


Figure 12.- Variation of $C_{l_{\beta C_L}}$ with Mach number.

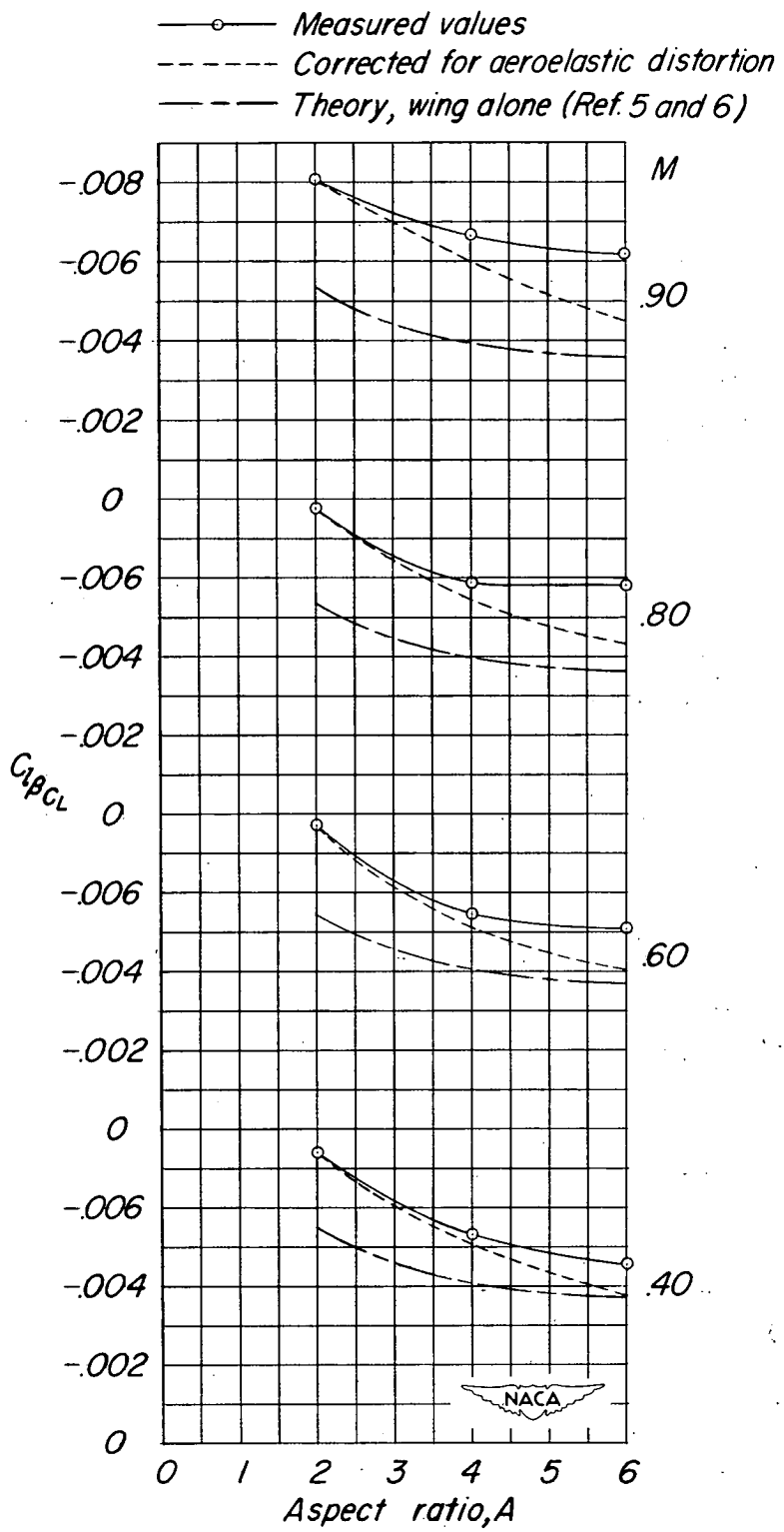


Figure 13.- Variation of $C_{l_{\beta C_L}}$ with aspect ratio.

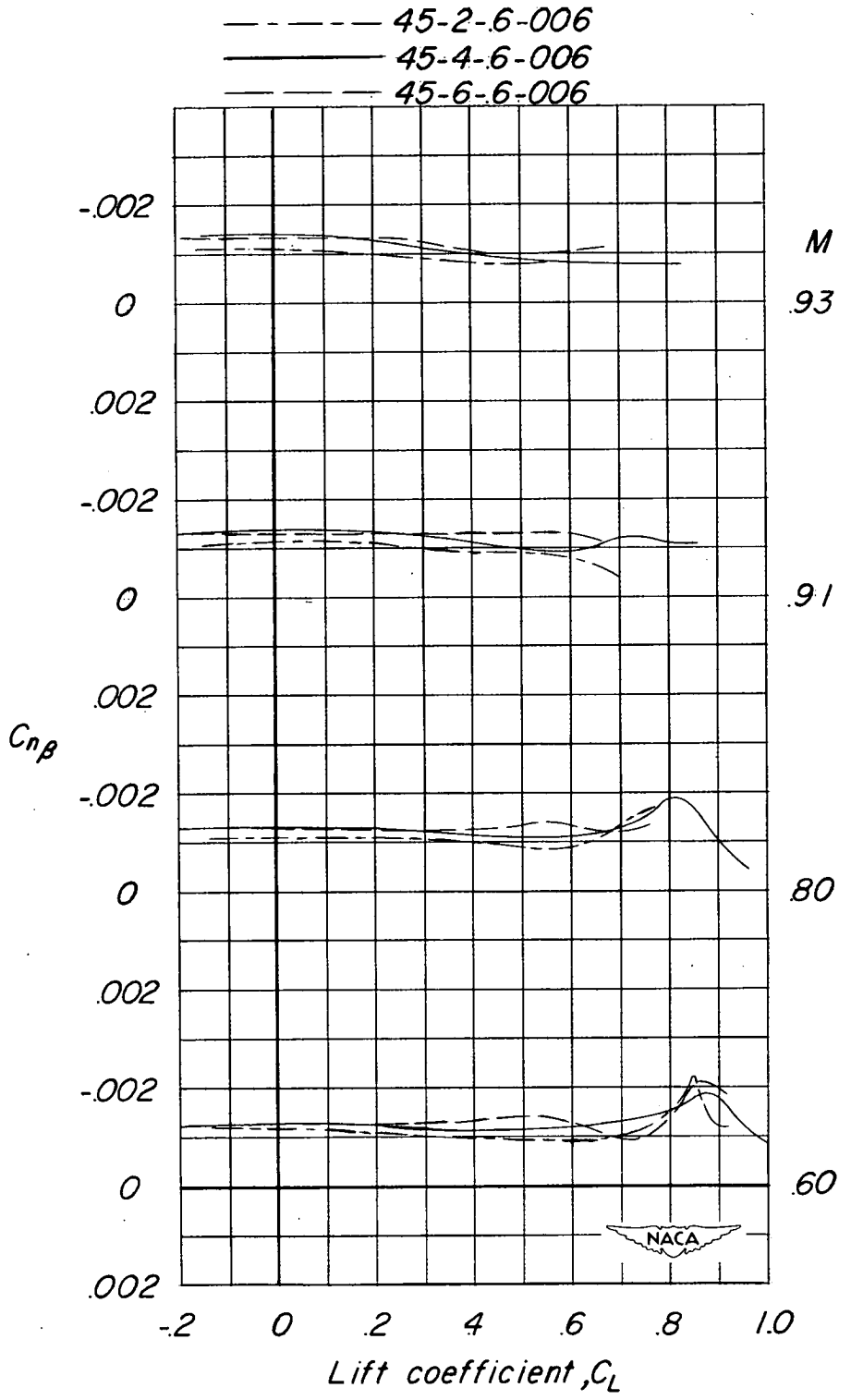


Figure 14.- Effects of aspect ratio on the variation of $C_{n_\beta}$ with lift coefficient for the wing-fuselage configurations at several Mach numbers.

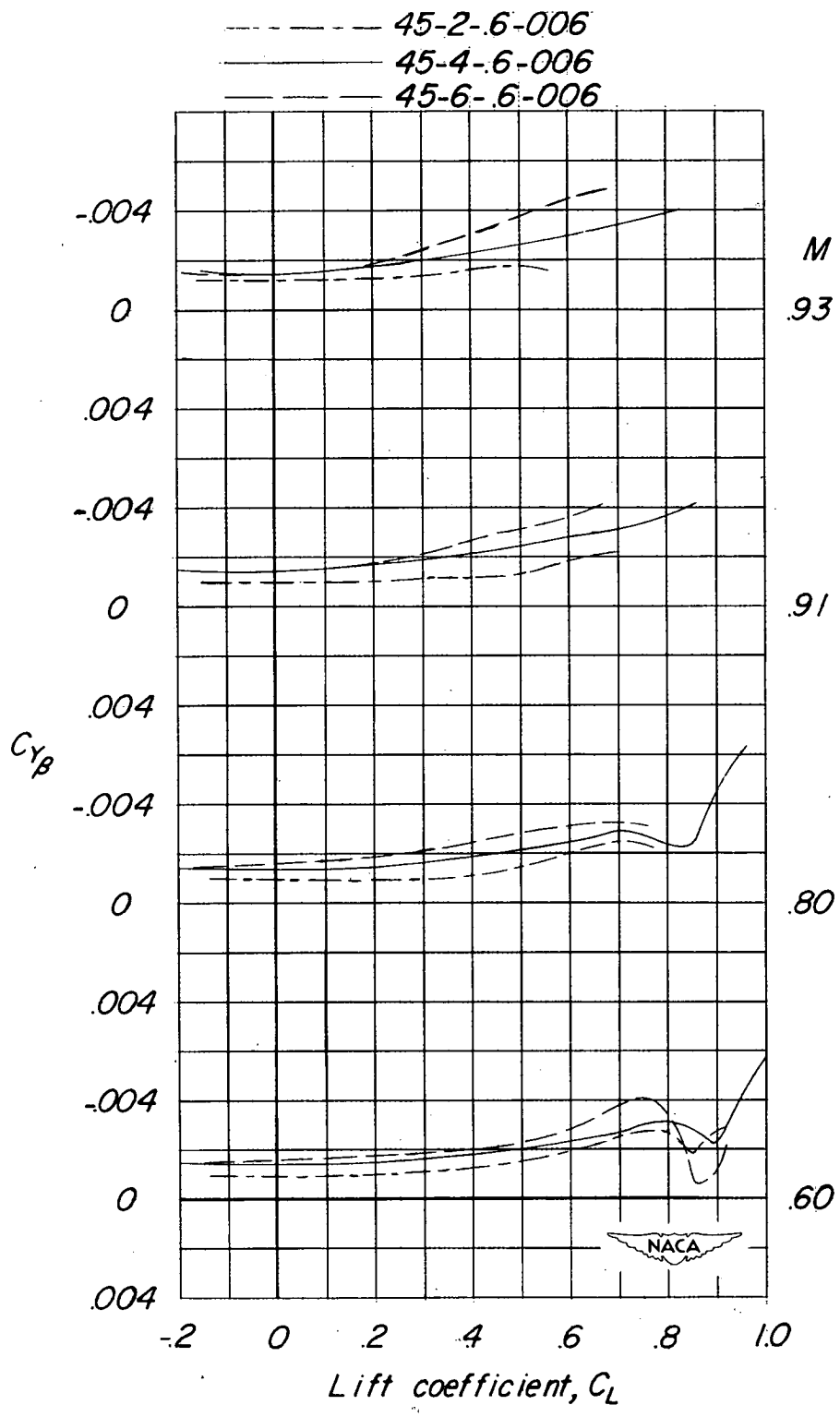


Figure 15.- Effects of aspect ratio on the variation of $C_{Y_\beta}$ with lift coefficient for the wing-fuselage configurations at several Mach numbers.

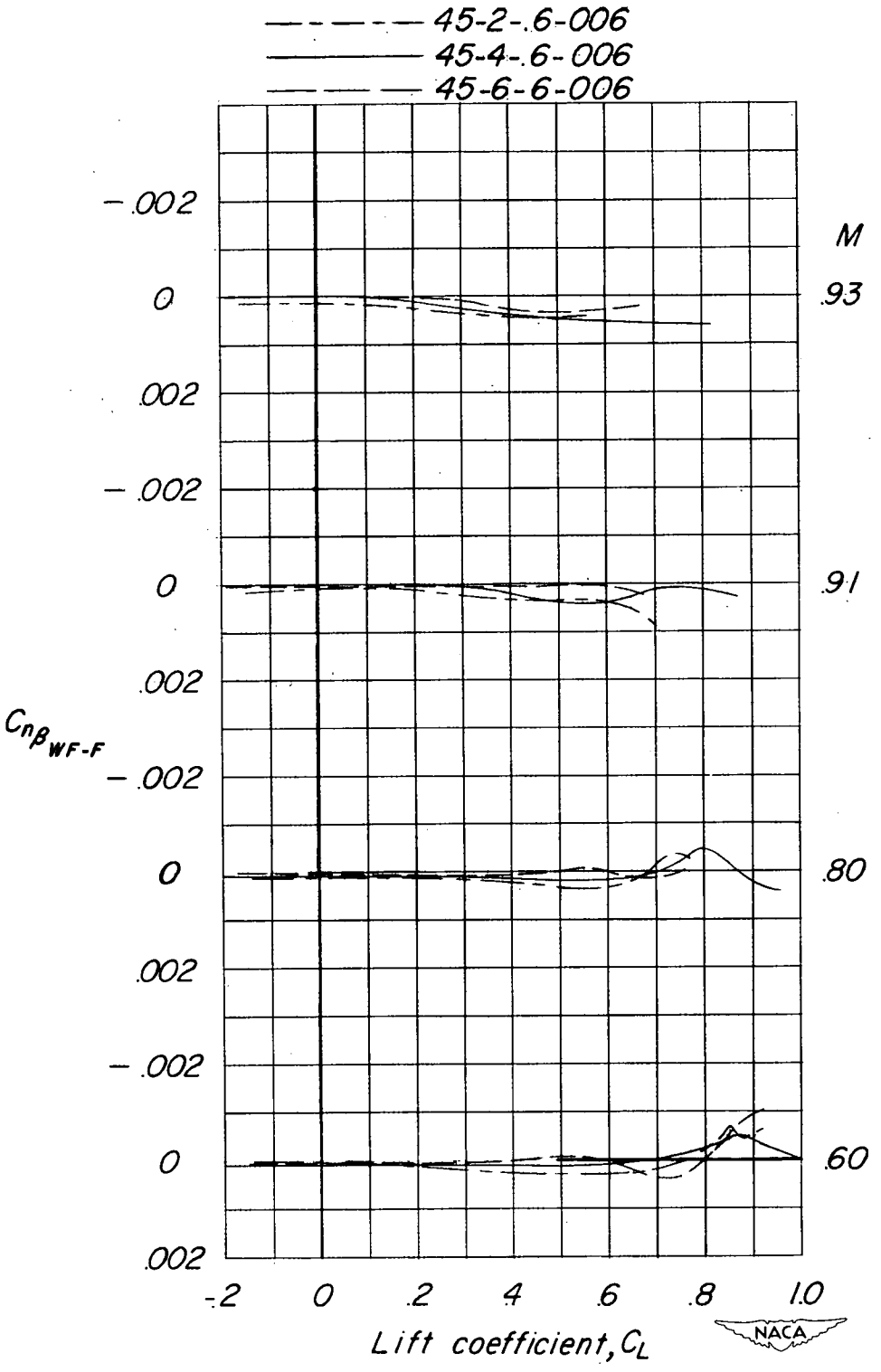


Figure 16.- Wing-plus-wing-fuselage-interference values of $C_{n_\beta}$ for the test wings compared at several Mach numbers.

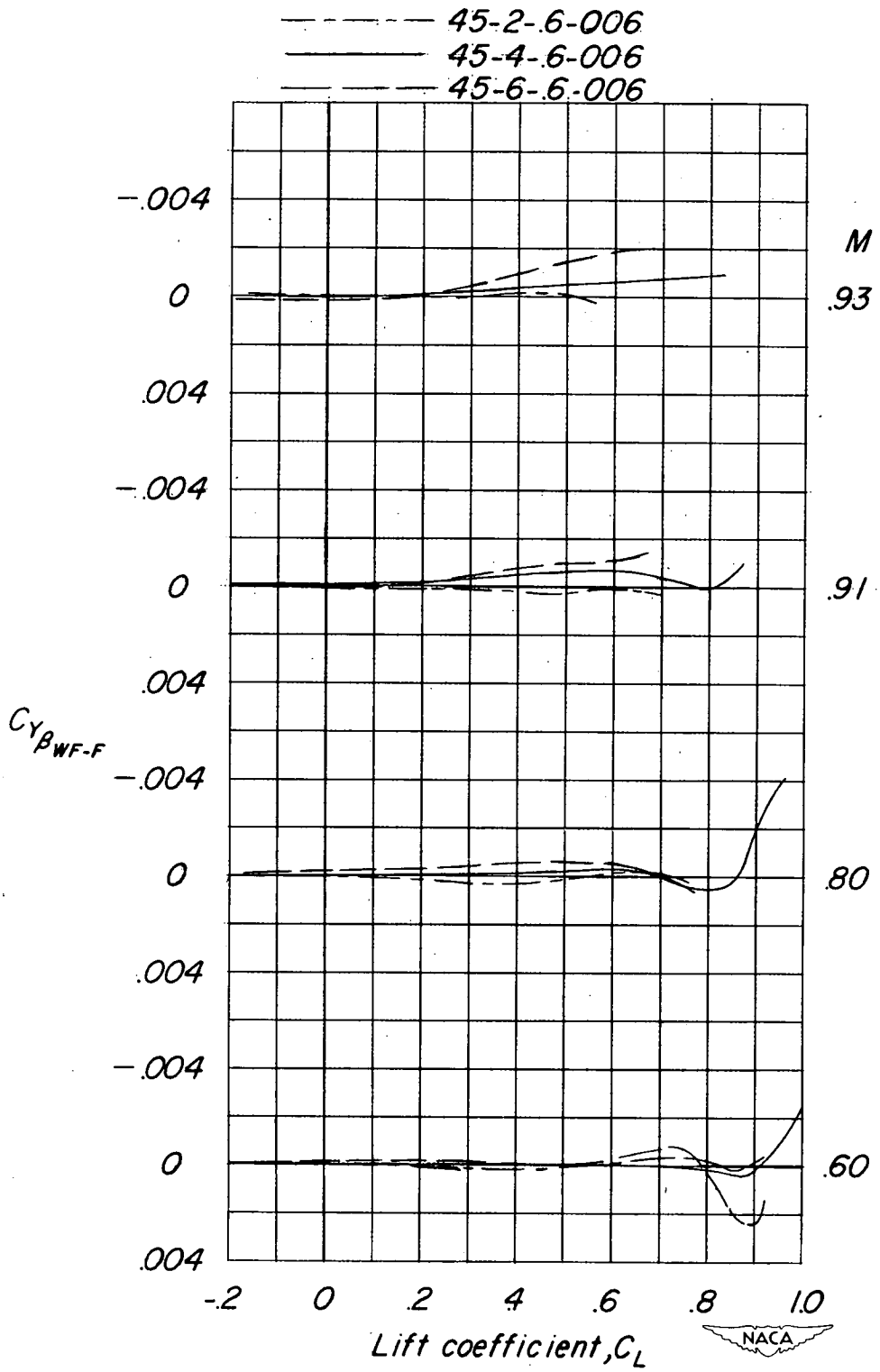


Figure 17.- Wing-plus-wing-fuselage-interference values of $C_{Y_\beta}$ for the test wings compared at several Mach numbers.